ELSEVIER

Chemistry & Biology 8 (2001) 379–389

Chemistry & Biology

www.elsevier.com/locate/chembiol

Research Paper

Mechanistic studies on the alkyltransferase activity of serotonin *N*-acetyltransferase

Weiping Zheng [a], Kara A. Scheibner [a], Anthony K. Ho [b], Philip A. Cole [a,*]

[a] *Department of Pharmacology and Molecular Sciences, The Johns Hopkins University School of Medicine, 725 North Wolfe Street, Baltimore, MD 21205, USA*

[b] *Department of Physiology, University of Alberta, Edmonton, AB, Canada T6G 2H7*

Received 19 January 2001; revisions requested 15 February 2001; revisions received 23 February 2001; accepted 27 February 2001
First published online 22 March 2001

Abstract

Background: Serotonin *N*-acetyltransferase (arylalkylamine *N*-acetyltransferase, AANAT) catalyzes the first, rate-limiting step in the biosynthesis of the circadian hormone melatonin (5-methoxy-*N*-acetyltryptamine) from serotonin. Our recent discovery that, in addition to catalyzing the acetyl transfer from acetyl-coenzyme A (acetyl-CoASH) to serotonin, AANAT is also a robust catalyst for the alkyl transfer reaction between CoASH and *N*-bromoacetyltryptamine has not only opened up a new way to develop cell-permeable AANAT acetyltransferase inhibitors that are valuable in vivo tools in helping elucidate melatonin's (patho)physiological roles, but has also raised a question – how does AANAT accelerate the alkyl transfer reaction? In this study, mechanistic aspects of the AANAT-catalyzed alkyl transfer reaction were explored by employing CoASH and a series of *N*-haloacetyltryptamines that were also evaluated for their AANAT acetyltransferase inhibitory activities.

Results: Investigation of various *N*-haloacetyltryptamine analogs showed a similar leaving group effect on the enzymatic and non-enzymatic reaction rates. Steady-state kinetic analyses demonstrated that AANAT alkyltransferase obeys a sequential, ternary complex mechanism, with random substrate binding. Rate versus pH profiles revealed the catalytic importance of an ionizable group with p$K_a \sim 7$. All those *N*-haloacetyltryptamines that serve as substrates of AANAT alkyltransferase are also potent (low micromolar) in vitro inhibitors against AANAT acetyltransferase activity. In particular, *N*-chloroacetyltryptamine was also shown to be a potent inhibitor of intracellular melatonin production in a pineal cell culture assay.

Conclusions: This is the first detailed investigation of the alkyltransferase activity associated with an acetyltransferase. Our results indicate that AANAT does not accelerate the alkyl transfer reaction by simple approximation effect as previously proposed for the similar alkyl transfer reaction catalyzed by other acyltransferases. This study has general implications for developing novel inhibitors by taking advantage of the promiscuous alkyltransferase activity associated with several acyltransferases.

Keywords: Arylalkylamine *N*-acetyltransferase; Alkyltransferase; Inhibition; Mechanism

1. Introduction

Serotonin *N*-acetyltransferase (arylalkylamine *N*-acetyltransferase, AANAT) catalyzes the first, rate-limiting step in the biosynthesis of the circadian hormone melatonin (5-methoxy-*N*-acetyltryptamine) from serotonin (Fig. 1) [1–5]. AANAT has received wide attention during past years for at least two reasons. First, although melatonin has been claimed to be effective in treating disorders ranging from insomnia to cancers to Alzheimer's disease, and in reversing the aging process, solid scientific foundation is still lacking for most of these claims, and physiological/pathophysiological roles played by melatonin are still unclear [6–14]. It is conceivable that AANAT, being the rate-

Abbreviations: AANAT, arylalkylamine *N*-acetyltransferase; GCN5, general control and non-repressed factor 5 (a yeast transcription factor and histone acetyltransferase); MES, 2-(*N*-morpholino)ethanesulfonic acid; MOPS, 3-(*N*-morpholino)propanesulfonic acid; EPPS, *N*-(2-hydroxyethyl)piperazine-*N*′-(3-propanesulfonic acid); DTNB, 5,5′-dithiobis-(2-nitrobenzoic acid); NMR, nuclear magnetic resonance; TLC, thin layer chromatography; GST, glutathione *S*-transferase; HPLC, high pressure liquid chromatography; CoASH, coenzyme A; EDC·HCl, 1-(3-dimethylaminopropyl)-3-ethylcarbodiimide hydrochloride

* Correspondence: Philip A. Cole;
E-mail: pcole@jhmi.edu

1074-5521/01/$ – see front matter
PII: S1074-5521(01)00020-5

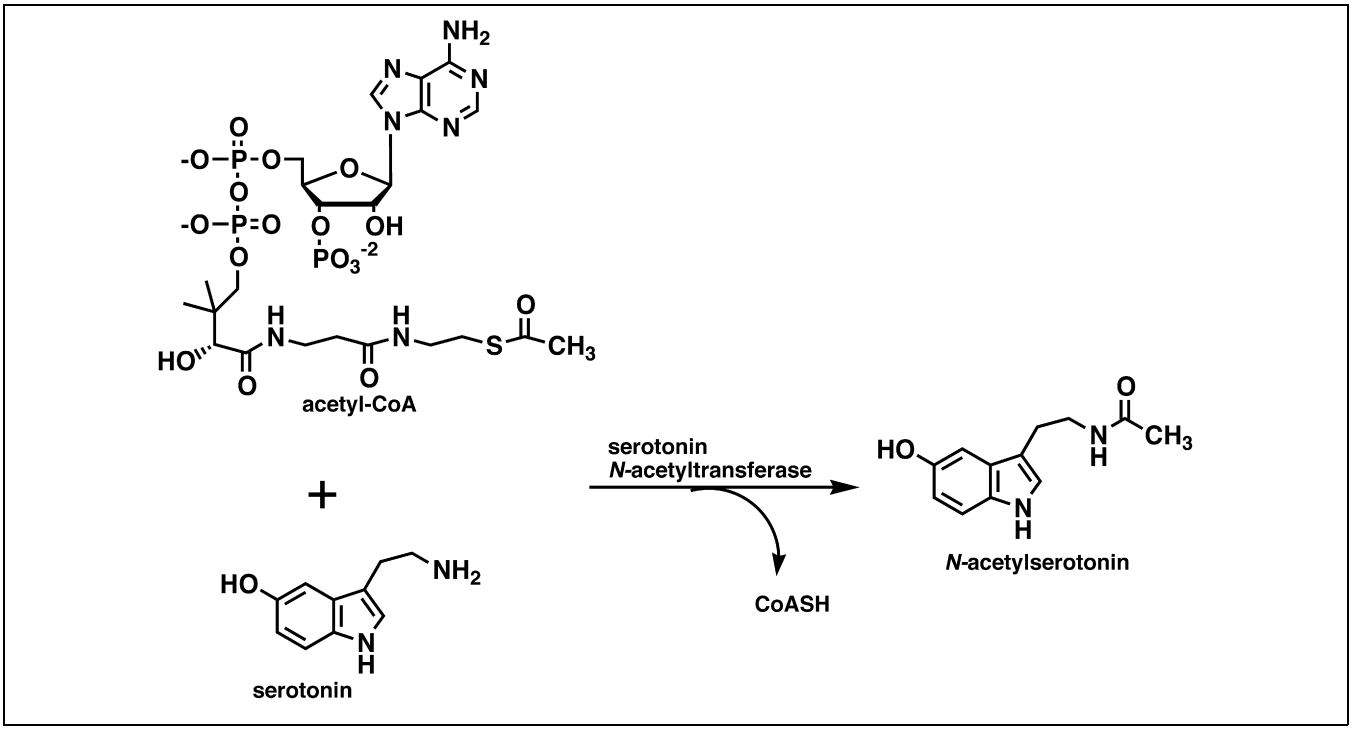

Fig. 1. AANAT-catalyzed acetyltransferase reaction.

limiting enzyme in the biosynthesis of melatonin, is a valuable target for developing potent, specific, and cell-permeable AANAT inhibitors to address the (patho)physiological relevance of melatonin. Second, AANAT belongs to the GCN5-related *N*-acetyltransferase superfamily [15] that also includes the aminoglycoside *N*-acetyltransferases, important in antibiotic resistance [16], and some histone *N*-acetyltransferases [17], important in chromatin remodelling and gene expression regulation. Recent mechanistic studies suggested that AANAT [18] and other superfamily members [19–22] obey sequential kinetic mechanisms and where determined, acetyl-coenzyme A (acetyl-CoASH) binds prior to the amine substrate.

Based on the sequential ordered Bi Bi kinetic mechanism of AANAT, we recently developed a potent bisubstrate analog inhibitor (**1**) (Figs. 2 and 3) [23,24]. However, due to its charged nature, compound **1** is predicted not to be cell-permeable [25], thus rendering it unsuitable for in vivo studies. Thanks to our recent discovery that, in addition to catalyzing the acetyl transfer from acetyl-CoASH to serotonin to form *N*-acetylserotonin, AANAT is also a robust catalyst for the alkyl transfer reaction between CoASH and *N*-bromoacetyl-tryptamine (**2**) to form the bisubstrate analog inhibitor **1** (Fig. 2), compound **2** was shown to be a potent AANAT acetyltransferase inhibitor in vitro and in vivo [24]. This latter inhibition was manifested by the fact that compound **2** inhibited the intracellular melatonin production in a pineal cell culture assay. The AANAT acetyltransferase inhibitory activity of compound **2** is believed to result from AANAT-catalyzed formation of the bisubstrate analog inhibitor **1** from CoASH and **2**, since compound **2** was clearly demonstrated not to be an affinity label of AANAT [24]. These previous studies have clearly brought about two issues of immediate importance, i.e. (i) how AANAT accelerates the alkyl transfer reaction described above, and (ii) how to exploit AANAT alkyltransferase activity to develop cell-permeable AANAT acetyltransferase inhibitors that are

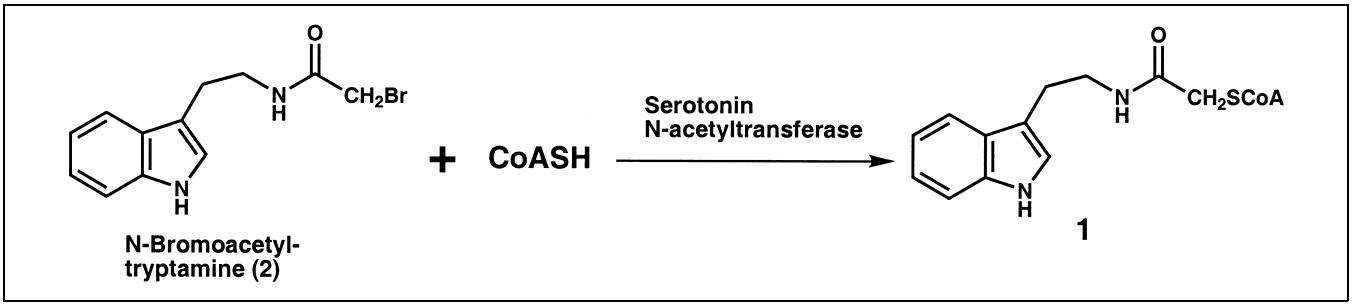

Fig. 2. Alkyl transfer reaction between CoASH and *N*-bromoacetyltryptamine (**2**).

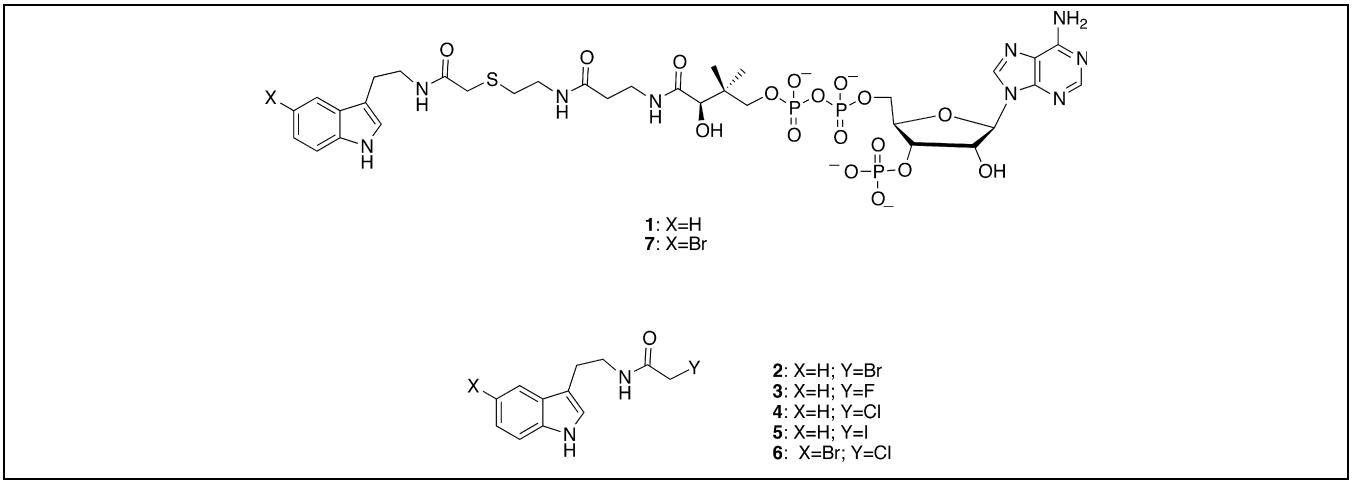

Fig. 3. Structures of compounds employed in this study.

superior to our lead compound **2**, since conceivably high intrinsic reactivity of compound **2** toward nucleophilic species may limit its utility in whole animal studies.

Two acetyltransferases have been previously reported to be able to catalyze the similar alkyl transfer reaction described above for AANAT [26–28]. These include carnitine acetyltransferase and gentamicin acetyltransferase I. However, it has remained unclear how these acyltransferases accelerate the secondary alkyl transfer reaction. In the case of AANAT, our previous studies suggested that the acetyltransferase and the alkyltransferase activities of AANAT are catalyzed at functionally distinct sites [24]. As such, different catalytic mechanisms are likely employed by these two transferase activities. In the current study, mechanistic aspects of the AANAT-catalyzed alkyl transfer reaction were explored by employing CoASH and a series of *N*-haloacetyltryptamines that were also evaluated for their AANAT acetyltransferase inhibitory activities. We have shown that AANAT alkyltransferase obeys a sequential, ternary complex mechanism, with random substrate binding. Our results also indicated that AANAT does not accelerate the alkyl transfer reaction by simple approximation effect as previously proposed for the similar alkyl transfer reaction catalyzed by other acyltransferases. We have also found that *N*-chloroacetyltryptamine (**4**, Fig. 3) was a potent in vitro and in vivo AANAT acetyltransferase inhibitor.

2. Results and discussion

2.1. Role of the leaving group

Among the first AANAT alkyltransferase reaction mechanistic features we planned to analyze was the role of the leaving group in the reaction. To address this issue, in addition to *N*-bromoacetyltryptamine (**2**), we have prepared *N*-fluoroacetyltryptamine (**3**), *N*-chloroacetyltryptamine (**4**), and *N*-iodoacetyltryptamine (**5**) using standard amide-bond-forming reactions between tryptamine and the corresponding halo-acetic acid (Fig. 3). These compounds were reacted with CoASH in the presence and absence of AANAT at pH 6.8. The second-order rate constants for the uncatalyzed reaction are shown in Table 1. As expected [29–32] (see below), the rate for iodide displacement involving **5** was similar (about two-fold faster) to that of the bromide displacement reaction with **2**, which in turn was 50-fold faster than the chloride reaction involving **4**. The fluoride displacement reaction employing **3** was undetectable. The AANAT-catalyzed alkyltransferase reactions showed similar overall trends in rate to the corresponding non-enzymatic reactions, as displayed in Table 1, but several differences were observed. The AANAT-catalyzed iodide displacement reaction involving **5** was slightly slower (two-fold) compared to the enzyme-catalyzed bromide displacement reaction. Most notably, the chloride

Table 1
Kinetic parameters for *N*-haloacetyltryptamines **2**–**6** as non-enzymatic and AANAT substrates for alkyl transfer to CoASH

N-Haloacetyltryptamine	Non-enzymatic (k)[a]	K_m (mM)	k_{cat} (min^{-1})	k_{cat}/K_m (mM^{-1} min^{-1})	k_{cat}/k^b_{uncat}
2	4.2×10^{-2}	3.6 ± 0.6	160 ± 11.5	45	3.3×10^{4}
3	$<10^{-6}$			<0.0013	
4	8.2×10^{-4}	1.7 ± 0.4	22 ± 1.7	13	2.2×10^{5}
5	7.4×10^{-2}	3.0 ± 0.7	83.7 ± 10.6	27.9	9.4×10^{3}
6		0.3 ± 0.07	14 ± 1.4	46.8	

[a]Second-order rate constant (M^{-1} s^{-1}).

[b]k_{uncat}, pseudo-first-order rate constant at fixed *N*-haloacetyltryptamine (2 mM).

displacement reaction with substrate **4** was only 7.4-fold lower in k_{cat} and about 3.5-fold smaller in k_{cat}/K_m compared to the AANAT-catalyzed alkyltransferase reaction involving the bromide substrate **2**. The enzyme-catalyzed displacement of fluoride in compound **3** was undetectable, similar to the non-enzymatic reaction.

The relative rate acceleration (k_{cat}/k_{uncat}) for alkyl transfer involving the chloride substrate **4** by AANAT is 2.2×10^5, which is almost an order of magnitude greater than that corresponding to reaction of the bromide substrate **2** (Table 1). In principle several possibilities could account for the greater relative enzymatic reactivity of chloride **4** compared to bromide **2**. For non-enzymatic S_N2 reactions, a body of work has demonstrated that the nature of the leaving group can significantly influence the rate [29–32]. The order of reactivity for halide leaving groups in these reactions is typically $I \geq Br > Cl \gg F$ [29–32]. However, for enzyme-catalyzed nucleophilic displacement reactions [33–35], the relative rate dependence on the leaving group may be different from the non-enzymatic cases for several reasons. First, the chemical step may not be rate-determining for the overall k_{cat}. For example, product release may be much slower than the chemical step and rate-determining for the overall reaction [36]. This could mask rate reductions due to substitutions with poorer leaving groups that would only impact the chemical step. Second, different leaving groups may bind specifically with active site residues. Such binding interactions could be affected by subtle changes in size and shape of the leaving groups, which may in turn influence the efficiency of catalysis. In general it is difficult to carry out a broad assessment of the effects on rate of varying the leaving group in enzyme-catalyzed nucleophilic displacement reactions because of geometric constraints. A homologous halide series in the AANAT case studied here, however, offers a more hopeful system than for example the pyrophosphate leaving group in prenyltransferases because subtle alterations of the pyrophosphate function are less apparent [33–35]. Third, the enzyme may alter the nature of the transition state by neutralizing charge build-up on the leaving group with a general acid group, or by influencing the reaction to proceed via a covalent enzyme intermediate over two chemical steps. Either of these effects could lessen the apparent importance of the leaving group on the overall reaction [37].

In our opinion, the best explanation for the rate effects with AANAT is that the chemical step is fully rate-determining for AANAT-catalyzed alkyl transfer reaction with chloride substrate **4**, whereas in the case with bromide substrate **2**, the chemical step is only partially rate-determining for the overall k_{cat}. Support for this assertion comes from studies on the alkyltransferase reaction catalyzed by [Y168F]-AANAT. Previous work by Hickman et al. showed that this tyrosine residue is important for the acetyltransferase reaction (the mutant showed about a 30-fold k_{cat} reduction with tryptamine as substrate) and its phenol hydroxyl is in hydrogen bonding distance to the sulfur atom of the bisubstrate analog **1** in an X-ray structure [38]. The same Y168F mutant was generated and used to investigate the alkyltransferase reaction. Interestingly, this Y168F mutant showed a k_{cat} (0.55 min^{-1}) which was 290-fold reduced in its catalysis of the alkyltransferase reaction with the bromide substrate **2**. In contrast, the reduction was 2200-fold with the chloride substrate **4** ($k_{cat} = 0.010$ min^{-1}). The reduction was 70-fold with Y168F and the iodide substrate **5** ($k_{cat} = 1.2$ min^{-1}).

These studies also suggested that the chemical step is rate-determining for [Y168F]-AANAT-catalyzed alkyl transfer reaction with all three substrates, i.e. iodide **5**, bromide **2**, and chloride **4**. This is evident from the fact that the ratio of apparent k_{cat} values for the [Y168F]-AANAT-catalyzed reactions (**5**:**2**:**4** = 120:55:1) is essentially identical to that for the non-enzymatic reactions (**5**:**2**:**4** = 90:51:1). This comparison also suggests that the extent of leaving group departure in the chemical step transition state is likely to be similar for AANAT-catalyzed and non-enzyme-catalyzed alkyl transfer reactions. From modelling studies it seems implausible that Tyr-168 can interact with the leaving halide atoms. Furthermore, even if Tyr-168 were stabilizing the departing halides, it would seem unlikely that it would preferentially stabilize chloride over bromide. For these reasons, we believe the simplest rationale for the chloride and bromide alkyltransferase rates with wild-type AANAT is that the chemical step is only partially rate-limiting with **2**, but fully rate-limiting with **4**. It is interesting that the Tyr-168 side chain is important for enhancing the AANAT alkyltransferase reaction, and we rationalize this role as due to a hydrogen-bonding interaction between CoASH and the phenol hydroxyl, orienting the CoASH substrate for attack.

2.2. *Steady-state kinetic analysis*

By employing CoASH and *N*-chloroacetyltryptamine (**4**) as substrates for the AANAT-catalyzed alkyl transfer reaction, steady-state kinetic analysis and rate versus pH experiments (see below) were performed. The choice of the chloride substrate **4** for these experiments was based on studies described above. Among the three substrates (**2**, **4**, and **5**), the chloride substrate **4** displayed the greatest enhancement in the AANAT-catalyzed versus uncatalyzed rate and therefore should provide a greater signal-to-noise ratio in a detailed kinetic analysis. Furthermore, since the chemical step (as opposed to product release) is rate-determining for the AANAT-catalyzed reaction with this substrate, use of the chloride compound **4** in kinetic studies is likely to lead to simpler interpretations.

While the AANAT-catalyzed acetyltransferase reaction proceeds via a sequential mechanism [18], it was formally possible that a covalent enzyme intermediate for the AANAT alkyltransferase reaction could occur, which would

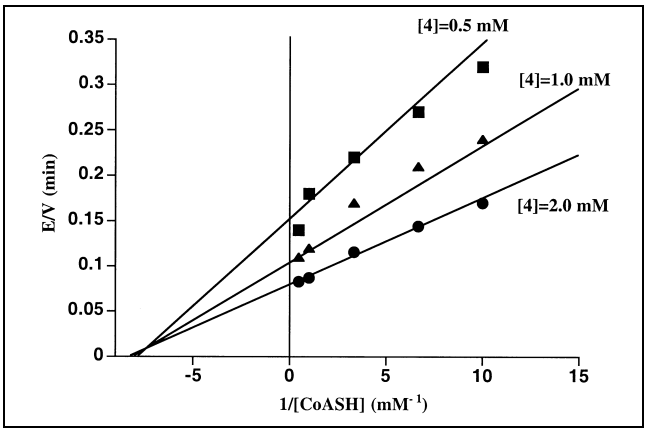

Fig. 4. Two-substrate kinetic analysis of AANAT alkyltransferase activity. *E*/*V* versus 1/[CoASH] at three fixed *N*-chloroacetyltryptamine (**4**) concentrations (0.5, 1, and 2 mM). Alkyltransferase assays and data fitting were performed as described in Section 4. The catalytic parameters are: k_{cat}, 18 ± 2 min^{-1}; K_m (CoASH), 0.11 ± 0.04 mM; K_m (**4**), 0.87 ± 0.19 mM; K_{ia} (CoASH), 0.13 ± 0.06 mM.

likely follow a ping-pong kinetic mechanism. To distinguish between these possibilities, a two-substrate kinetic analysis was performed [39]. In this experiment, a clear intersecting line pattern as opposed to a parallel line pattern was observed (Fig. 4). This suggests that the AANAT-catalyzed alkyltransferase reaction proceeds via a sequential mechanism, and a direct attack of CoASH on **4** is expected.

The next question concerning the kinetic mechanism was whether substrate binding of CoASH and **4** follows a random pathway or whether ordered binding of one substrate prior to the other occurs. AANAT-catalyzed acetyltransferase activity shows an ordered Bi Bi kinetic mechanism in which acetyl-CoASH binding precedes serotonin (or tryptamine) binding [18]. One criterion for the ordered Bi Bi classification was the finding that the bisubstrate analog **1** was a competitive inhibitor versus acetyl-CoASH and a non-competitive inhibitor versus tryptamine [23,24]. In the current work, we carried out analogous studies with the bisubstrate analog inhibitor **7** (Fig. 3), also a close analog of the direct product (**1**) for the reaction between CoASH and the chloride substrate **4**. Compared to **1**, compound **7** shows slightly increased (2–4-fold) potency with regard to inhibiting AANAT acetyltransferase and alkyltransferase activity [24]. More important for this work, it is well separated from **1** (**7** shows about 2 min increased retention time) under the high pressure liquid chromatography (HPLC) assay conditions used here and does not interfere with quantitative analysis of the alkyltransferase activity.

When the inhibition pattern of analog **7** for the AANAT-catalyzed alkyltransferase reaction was analyzed, **7** was found to be a linear competitive inhibitor versus both CoASH and substrate **4** (Fig. 5). The measured K_{is} extrapolated to zero concentration of both substrates was $\sim$700 nM, which should be equal to the K_d for **7** with respect to the alkyltransferase active site. This pattern of inhibition differs from the pattern observed with bisubstrate analog inhibition of the AANAT acetyltransferase reaction and suggests that substrates CoASH and **4** bind to AANAT randomly for the alkyltransferase reaction.

The finding of the difference in the order of substrate binding for the AANAT acetyltransferase and alkyltransferase reactions is compatible with the possibility that the alkyltransferase reaction takes place in a separate and conformationally altered active site on AANAT compared to the acetyltransferase reaction [24]. A comparison of the approximate K_d values for the acetyltransferase site (22 nM) [24] versus the alkyltransferase site (700 nM) by the same molecule **7** is also consistent with this possibility. How these conformationally altered active sites arise is unknown but they may represent differences within an asymmetric homodimer of the AANAT protein as has been discussed previously [24].

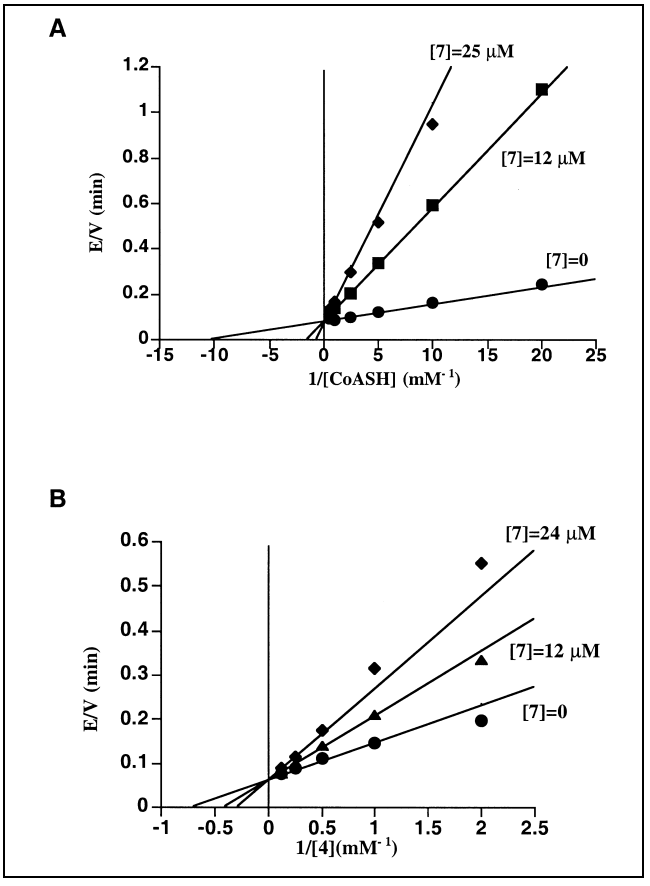

Fig. 5. Bisubstrate analog **7** inhibition of AANAT alkyltransferase activity. (A) *E*/*V* versus 1/[CoASH] at fixed *N*-chloroacetyltryptamine (**4**) concentration (4 mM) and varying concentrations of bisubstrate analog **7** (0, 12, and 25 μM). The catalytic parameters are: k_{cat}, 12 ± 0.2 min^{-1}; K_m (CoASH), 0.088 ± 0.008 mM; K_{is} (**7**), 2.1 ± 0.2 μM. (B) *E*/*V* versus 1/[**4**] at fixed CoASH (2 mM) and varying concentrations of **7** (0, 12, and 24 μM). The catalytic parameters are: k_{cat}, 16 ± 1 min^{-1}; K_m (**4**), 1.3 ± 0.1 mM; K_{is} (**7**), 17 ± 3 μM. Alkyltransferase assays and data fitting were performed as described in Section 4.

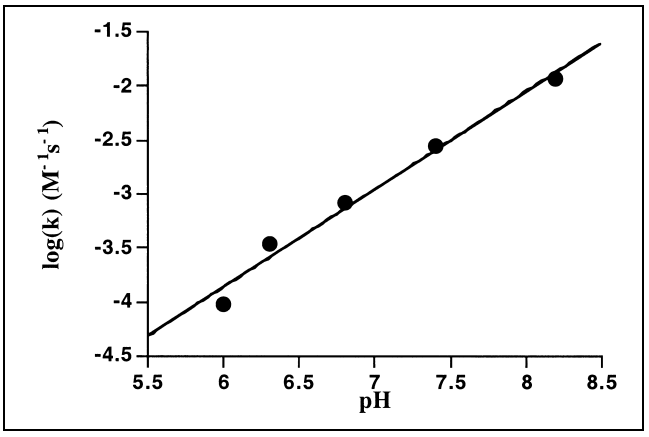

Fig. 6. Non-enzymatic rate of alkyl transfer reaction between CoASH and **4** as a function of pH. These reactions were carried out with fixed CoASH (2 mM) and **4** (2 mM) concentrations as described in Section 4. It has been shown previously that the reaction is second order with respect to both substrates in this concentration range [24]. The vertical axis represents the log(k) where k is the second-order rate constant (M^{-1} s^{-1}). Data were fitted using a least squares linear model (slope = +0.91 ± 0.07)

2.3. *Effects of pH changes on the alkyltransferase activity*

It was unclear if AANAT's alkyl transfer rate enhancement is due solely to a simple approximation effect, bringing the two substrates close together, or if enzyme active site residues are directly facilitating the reactions with hydrogen bonding or general base catalysis. In the non-enzymatic reaction, the thiolate anion of CoASH would be expected to be the active nucleophilic species and this alkyl transfer reaction should be accelerated by base catalysis. Indeed, pH titration of the non-enzymatic reaction rate shows that log(k) versus pH is linear with a slope near 1 (+0.91 ± 0.07) in the pH range 6–8.2 (Fig. 6). The pK_a of the CoASH thiol has been reported to be 9.6 [40] and therefore one would expect that the rate of the non-enzymatic reaction would not plateau until approaching pH 9.6.

In contrast, the pH–rate profile of the AANAT-catalyzed alkyltransferase reaction (log(k_{cat}) versus pH) shows an 'acidic limb' which plateaus around pH 8 (Fig. 7A). Fitting of these data to a model with a single titrating functionality provides evidence for an ionizable group with pK_a = 7.1 in which the deprotonated form is the active species. Since plots of log(k_{cat}) versus pH should reflect the pK_a values of important catalytic groups in the bound complex of enzyme plus substrate(s) [41], this ionizable group is likely to be either the CoASH thiol or an acid–base functionality on an enzyme residue. Due to signal-to-noise limitations, it was not possible to carry out reliable pH–rate measurements on [Y168F]-AANAT, and the contributions of this residue could not be assessed. Although the pK_a from the wild-type AANAT reaction is much lower than that of the CoASH thiol, it is well known that protein active sites can alter the pK_a values of ionizable groups on ligands compared to their values in free solution. These pK_a changes can result from hydrogen bonding, dielectric constant changes, or electrostatic effects. Interestingly, the log(k_{cat}/K_m-CoASH) versus pH plot, which should reflect acid–base groups on the unbound enzyme or free substrates [41], shows a similar profile with a single ionizable group with pK_a = 6.4, near the value of 7.1 for the k_{cat} profile (Fig. 7B). In this case, this plot presumably represents a pK_a value of a group on an enzyme residue in the unbound form, since the CoASH thiol pK_a is 9.6 in free solution [40] and *N*-chloroacetyltryptamine lacks ionizable groups. It is unlikely to be re-

Table 2
Steady-state kinetic parameters for *N*-haloacetyltryptamines (**2**–**6**) as inhibitors of the acetyltransferase activity of AANAT

N-Haloacetyltryptamine	IC_{50} (μM)
2	0.5
3	3700
4	5.2
5	1.3
6	6.5

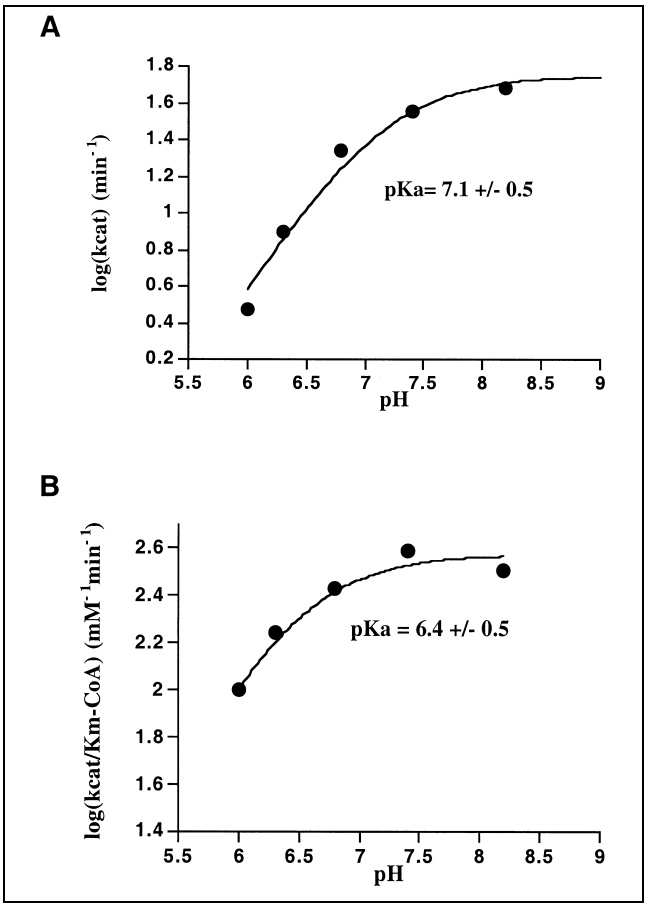

Fig. 7. AANAT-catalyzed alkyltransferase activity as a function of pH. (A) log(k_{cat}) versus pH. (B) log(k_{cat}/K_m (CoASH)) versus pH. Each of these plots was fit to reflect a single ionizable group which is active only in the deprotonated form with pK_a = 7.1 for k_{cat} and pK_a = 6.4 for k_{cat}/K_m. See Section 4 for details.

lated to the 3′-phosphate of CoASH which is not critical for CoASH binding [24].

There are two possible interpretations for the pH–rate profile results of the AANAT-catalyzed alkyltransferase reaction. Firstly, the key catalytic ionizable group in both the free and bound complex is the same and therefore corresponds to an enzymatic residue side chain. In this scenario, it is reasonably predicted to be a general base catalyst which assists in the proton removal of the CoASH thiol proton, activating it for nucleophilic attack. This proton transfer could occur either directly or through intervening water molecules [38]. Of note, there appears to be an ionizable group, as yet unidentified, with a similar pK_a that is important for AANAT acetyltransferase catalysis, possibly as a general base [42]. Another possibility, although somewhat more complicated, is that the ionizable group detected in the free enzyme is different from the group with a similar pK_a in the bound complex. In this scenario, the group in the bound complex might then be the CoASH thiol in which its pK_a falls 2.5 units in the environment of the enzyme active site. However, in either case, these data suggest that AANAT uses chemical groups to directly enhance the S_N2 reaction. In the first case this occurs by assisting proton transfer in the transition state and in the second case by increasing the proportion of the powerful nucleophile thiolate anion at neutral pH.

2.4. Acetyltransferase inhibition

Our recent discoveries that, in addition to catalyzing the acetyl transfer from acetyl-CoASH to serotonin, AANAT is also a robust catalyst for the alkyl transfer reaction between CoASH and *N*-bromoacetyltryptamine (**2**), as well as that compound **2** was shown to be a potent AANAT acetyltransferase inhibitor in vitro and in vivo [24] have placed AANAT alkyltransferase activity in a central position for developing cell-permeable AANAT acetyltransferase inhibitors by pharmacologically exploiting the alkyltransferase reaction. In this regard, it was worthwhile to attempt to correlate the acetyltransferase inhibitory potency of compounds **2**–**5** with respect to their alkyltransferase substrate activity in vitro. As can be seen in Table 2, the acetyltransferase inhibitory potency correlated fairly well with the alkyltransferase substrate activity. As expected, chloride **4** ($IC_{50} = 5.2$ μM) was less potent than bromide **2** ($IC_{50} = 0.5$ μM) in blocking AANAT acetyltransferase activity in vitro. Because of a short incubation time (4 min), this in vitro acetyltransferase inhibition screening assay is somewhat biased in favor of a halide compound which can undergo more rapid alkyltransferase reaction. A more biologically relevant assay in which melatonin production is measured in pineal cells can also be employed. Indeed, in the pinealocyte melatonin production assay which takes place over a much longer time period (6 h), the IC_{50} values for **4** (∼500 nM, see Table 3) and **2** (∼200–400 nM, see [24]) were fairly similar. Other parameters which impact bioavailability such as cell entry, protein binding, and metabolic stability will also affect the comparison in cell culture assays as well as animal studies [43]. Because of its reduced spontaneous rate of reacting with nucleophiles compared to bromide **2**, chloride **4** can plausibly be expected to have more favorable pharmacokinetic behavior compared to **2**.

Table 3
Inhibition of melatonin production in pinealocytes by *N*-chloroacetyltryptamine (**4**)

Treatment	Melatonin (pmol/10^5 cells)
Background	0.60 ± 0.03
4 (85 μM)	0.12 ± 0.05
NE (10 μM)[a]	15.37 ± 0.41
NE (10 μM)+**4** (85 μM)	3.39 ± 0.25
NE (10 μM)+**4** (8.5 μM)	3.56 ± 0.61
NE (10 μM)+**4** (0.85 μM)	6.07 ± 0.73

[a]NE = norepinephrine. $N = 3$. $IC_{50} \sim 0.5$ μM. See [24] for experimental details.

To further explore the design of acetyltransferase inhibitors, we investigated compound **6** (Fig. 3) as an alkyltransferase substrate (Table 1) and acetyltransferase inhibitor (Table 2). It was reported previously that bromo-substituted bisubstrate analog **7** is a somewhat more potent acetyltransferase inhibitor (ca. two-fold) compared to the parent bisubstrate analog **1** [24]. Moreover, it was recently shown that 5-bromotryptamine is a five-fold more efficient substrate for AANAT acetyltransferase processing ($k_{cat} = 25$ s^{-1}, $K_m = 0.03$ mM; unpublished data from the Cole laboratory), compared to serotonin or tryptamine. It was of interest to determine whether 5-bromo substitution would lead to enhanced AANAT alkyltransferase processing of **6**. Indeed, **6** was a more efficient alkyltransferase substrate than **4** (Table 1) and the effect was solely a K_m rather than a k_{cat} effect. This suggests that the acetyltransferase binding site for 5-bromo-tryptamine shares structural homology with the alkyltransferase binding site for 5-bromo-*N*-chloroacetyltryptamine. Despite this, **6** did not show enhanced acetyltransferase inhibition properties compared to **4** (Table 2) in the in vitro assay. The IC_{50} values were indistinguishable within the standard error of the measurement. While the reasons for this lack of enhanced potency for **6** are not fully known, it suggests that the k_{cat} of the alkyltransferase reaction is more important than the K_m as a predictor for potent inhibition in the in vitro acetyltransferase assay. Due to the cross-reactivity with melatonin, compound **6** could not properly be assessed for the blockade of intracellular melatonin production in the pineal cell culture assay.

3. Significance

Although alkylation catalysis has been documented for

several acyltransferases, including AANAT, it has remained unclear how these acyltransferases accelerate the secondary (promiscuous) alkyl transfer reaction. In the current study, mechanistic aspects of AANAT alkyltransferase activity were examined by employing CoASH and a series of *N*-haloacetyltryptamines. We have shown that the leaving group ability is an important determinant of AANAT-catalyzed alkylation rate as it is for the non-enzymatic rate. Steady-state kinetic analyses demonstrated that AANAT alkyltransferase obeys a sequential, ternary complex mechanism, with random substrate binding. Rate versus pH profiles suggested that general base catalysis or the lowering of CoASH thiol pK_a is important for AANAT alkyltransferase reaction. These mechanistic studies should constitute an important contribution to understanding enzyme promiscuity. We have also shown that the in vitro AANAT acetyltransferase inhibitory potency of *N*-haloacetyltryptamines correlated well with their alkyltransferase substrate activities. In particular, *N*-chloroacetyltryptamine (**4**) was also shown to be a potent in vivo AANAT acetyltransferase inhibitor, as manifested by its potent inhibition of intracellular melatonin production in a pineal cell culture assay. Due to its lower spontaneous reactivity toward nucleophiles compared to **2**, compound **4** is expected to have more favorable pharmacokinetic behavior and should find applications in in vivo circadian research. This study should have general implications for developing novel inhibitors by taking advantage of the promiscuous alkyltransferase activity associated with several acyltransferases.

4. Materials and methods

4.1. General

5-Bromotryptamine hydrochloride was purchased from Biosynth Technologies (Skokie, IL, USA). CoASH, 2-(*N*-morpholino)ethanesulfonic acid (MES), 3-(*N*-morpholino)propanesulfonic acid (MOPS), *N*-(2-hydroxyethyl)piperazine-*N*′-(3-propanesulfonic acid) (EPPS), cysteine, 5,5′-dithiobis-(2-nitrobenzoic acid) (DTNB), and assay-grade tryptamine hydrochloride were purchased from Sigma. Acetyl-CoASH was purchased from Pharmacia Biotech. Sodium phosphate, guanidinium hydrochloride, and EDTA were purchased from Fisher Scientific. All other reagents were purchased from Aldrich. All commercially available reagents were used as purchased without further purification. Preparations of *N*-bromoacetyltryptamine (**2**) and bisubstrate analog inhibitors **1** and **7** have been described previously [23,24]. ^{1}H and ^{13}C nuclear magnetic resonance (NMR) spectra were obtained with a Bruker AMX 300 spectrometer (300 and 75.5 MHz, respectively), and chemical shift values (δ) were expressed as ppm relative to tetramethylsilane. Elemental analyses were performed by Robertson Microlit Laboratories (Madison, NJ, USA), and the values found were within ±0.4% of the theoretical values. Silica gel (Merck, 63–200 mesh, 60 Å) was used for the flash column chromatography. Analytical thin layer chromatography (TLC) was performed on Sigma-Aldrich silica gel 60 F 254 TLC plates (thickness: 200 μm). The preparation of recombinant sheep glutathione *S*-transferase (GST)–AANAT (∼90% pure) which was expressed in *Escherichia coli* has been described previously, and it has been shown that nearly identical acetyltransferase kinetic behavior was observed for GST–AANAT and GST-free AANAT [18]. GST–AANAT and GST-free AANAT were also shown to have essentially identical alkyltransferase kinetic behavior with the bromide compound **2** [24]. In particular the GST domain is unable to catalyze the AANAT alkyltransferase reactions [24]. Therefore, GST–AANAT was used for all the studies described in this manuscript.

4.2. Synthesis of N-fluoroacetyltryptamine (3)

To a well-stirred, ice-cooled two-phase solution of tryptamine (3.2 g, 20 mmol) and sodium fluoroacetate (2.2 g, 22 mmol) in a mixture of 0.5 M HCl (44 ml), methylene chloride (200 ml), and water (15 ml) was added in small portions 1-(3-dimethylaminopropyl)-3-ethylcarbodiimide hydrochloride (EDC·HCl; 4.22 g, 22 mmol). After the addition was complete, the reaction mixture was stirred vigorously at room temperature overnight. The organic layer was isolated, washed with water, and concentrated. The residue was dissolved in freshly degassed (45 min with N_2) MeOH (125 ml), and was treated with a solution of L-cysteine (665 mg, 5.5 mmol) in 1.0 M triethyl-ammonium bicarbonate buffer (pH 8.5, 125 ml). After being stirred at room temperature overnight, the solution was concentrated, and extracted with methylene chloride. The organic extract was washed with water, 0.5 M HCl, 1.0 M $NaHCO_3$, brine, and dried over anhydrous Na_2SO_4. Removal of solvents gave a white solid which was crystallized in methylene chloride/hexane, affording 694 mg (16%) of **3** as white crystals. ^{1}H NMR ($CDCl_3$) δ 8.09 (bs, 1H), 7.62 (d, J = 7.8 Hz, 1H), 7.39 (d, J = 8.0 Hz, 1H), 7.23 (t, J = 7.1 Hz, 1H), 7.14 (t, J = 7.1 Hz, 1H), 7.06 (s, 1H), 6.4 (bs, 1H), 4.77 (d, J = 47.1 Hz, 2H), 3.69 (q, J = 6.5 Hz, 2H), 3.03 (t, J = 6.8 Hz, 2H); ^{13}C NMR ($CDCl_3$) δ 167.6, 136.4, 127.1, 122.2, 122.0, 119.4, 118.5, 112.3, 111.3, 81.1, 79.3, 39.0, 25.2. Anal. calcd. for $C_{12}H_{13}N_2OF$: C, 65.44; H, 5.95; N, 12.72. Found: C, 65.29; H, 5.90; N, 12.73.

4.3. Synthesis of N-chloroacetyltryptamine (4)

To a stirred, ice-cooled suspension of tryptamine (160 mg, 1.0 mmol) and chloroacetic acid (104 mg, 1.1 mmol) in methylene chloride (15 ml) was added in small portions EDC·HCl (211 mg, 1.1 mmol). After the addition was complete, the reaction mixture was stirred at room temperature overnight. The organic layer was isolated, and the aqueous layer was extracted once with methylene chloride. The combined organic was washed with 0.5 M HCl, 1.0 M $NaHCO_3$, water, brine, and dried over anhydrous Na_2SO_4. Removal of solvents gave a white solid which was crystallized in methylene chloride/hexane, affording 211.4 mg (89%) of **4** as white crystals. ^{1}H NMR ($CDCl_3$) δ 8.09 (bs, 1H), 7.62 (d, J = 7.8 Hz, 1H), 7.39 (d, J = 8.1 Hz, 1H), 7.23 (t, J = 7.2 Hz, 1H), 7.15 (t, J = 7.8 Hz, 1H), 7.07 (s, 1H), 6.67 (bs, 1H), 4.02

(s, 2H), 3.65 (q, $J = 6.5$ Hz, 2H), 3.03 (t, $J = 6.7$ Hz, 2H); ^{13}C NMR ($CDCl_3$) δ 165.8, 136.4, 127.1, 122.3, 122.0, 119.6, 118.6, 112.5, 111.3, 42.7, 40.0, 25.1. Anal. calcd. for $C_{12}H_{13}N_2ClO$: C, 60.89; H, 5.54; N, 11.83. Found: C, 60.80; H, 5.45; N, 11.82.

*4.4. Synthesis of N-iodoacetyltryptamine (**5**)*

In the same manner as compound **4**, tryptamine (160 mg, 1.0 mmol) was coupled with iodoacetic acid (204.5 mg, 1.1 mmol) in the presence of 1-(3-dimethylaminopropyl)-3-ethylcarbodiimide methiodide (327 mg, 1.1 mmol), affording 95.7 mg (29%) of **5** as a white powder after flash silica gel chromatography (EtOAc/hexane = 1/3 → 1/1). ^{1}H NMR (DMSO-d_6) δ 10.81 (bs, 1H), 8.33 (bs, 1H), 7.52 (d, $J = 7.8$ Hz, 1H), 7.33 (d, $J = 8.1$ Hz, 1H), 7.15 (s, 1H), 7.06 (t, $J = 7.8$ Hz, 1H), 6.97(t, $J = 7.8$ Hz, 1H), 3.63 (s, 2H), 3.27–3.40 (m, 2H), 2.81 (t, $J = 7.2$ Hz, 2H). ^{13}C NMR (DMSO-d_6) δ 167.5, 136.2, 127.1, 122.8, 120.9, 118.3, 118.2, 111.5, 111.4, 40.0, 24.8, 12.1. Anal. calcd. for $C_{12}H_{13}N_2OI$: C, 43.92; H, 3.99; N, 8.54. Found: C, 44.00; H, 3.98; N, 8.47.

*4.5. Synthesis of 5-bromo-N-chloroacetyltryptamine (**6**)*

In the same manner as compound **4**, starting from 5-bromotryptamine hydrochloride (82.7 mg, 0.3 mmol), chloroacetic acid (31.2 mg, 0.33 mmol), and EDC·HCl (63.3 mg, 0.33 mmol) in the presence of Et_3N (47.4 µl, 0.34 mmol), 70 mg (74%) of **6** was obtained as white crystals after crystallization from methylene chloride/hexane. ^{1}H NMR (DMSO-d_6) δ 11.04 (bs, 1H), 8.29 (bs, 1H), 7.71 (s, 1H), 7.30 (d, $J = 8.6$ Hz, 1H), 7.21 (s, 1H), 7.16 (d, $J = 8.6$ Hz, 1H), 4.04 (s, 2H), 3.27–3.38 (m, 2H), 2.80 (t, $J = 7.5$ Hz, 2H); ^{13}C NMR (DMSO-d_6) δ 165.8, 134.9, 129.1, 124.5, 123.4, 120.6, 113.4, 111.5, 111.0, 42.7, 39.8, 24.6. Anal. calcd. for $C_{12}H_{12}N_2BrClO$: C, 45.67; H, 3.83; N, 8.88. Found: C, 45.67; H, 3.67; N, 8.90.

4.6. AANAT alkyltransferase assays of N-haloacetyltryptamines

A HPLC assay was performed to measure the rate of product (bisubstrate analog **1** or **7**) formation in the presence and absence of AANAT, as described previously [24]. Briefly, the assay reactions (pH 6.8) were quenched with a 6 M aqueous guanidinium hydrochloride solution (pH 3.0), and the whole mixtures were subjected to analytical reverse-phase HPLC analysis on a C-18 column (100 Å, 0.46 × 25 cm) to identify and quantify the reaction product (bisubstrate analog **1** or **7**) by automated integration using authentic synthetic materials as standards. Chromatograms were obtained by eluting the column with a gradient of 50 mM aqueous potassium phosphate buffer (pH 4.5) (mobile phase A) and MeOH (mobile phase B) (0–3 min, 0% B; 3–15 min, linear increase to 65% B; 15–20 min, linear increase to 100% B; 20–26 min, linear decrease to 0% B) (1 ml/min), and UV monitoring at 260 and 279 nm. Under these conditions, the following retention times were obtained: CoASH, 11 min; **1**, 15 min; **2**, 19 min; **3**, 18 min; **4**, 19 min; **5**, 21 min; **6**, 21 min; **7**, 17 min. The kinetic behavior of bromide **2** with AANAT has been characterized previously, and shows second-order kinetics in the 2 mM concentration range in the absence of enzyme [24]. Stock solutions of **3**–**6** were prepared in a mixture of propylene glycol (PG) and doubly distilled water (33–56% of PG (v/v)), and the final PG concentration in an assay reaction was maintained at $\leq 10\%$ (v/v). All assay reactions were performed at 30°C, and were initiated with the addition of potential *N*-haloacetyl-tryptamine substrates. Typical progress curves were obtained with the use of 2 mM of CoASH and 2 mM of *N*-haloacetyltryptamines in the presence and absence of 0.5–50 µM of AANAT. Linearity was obtained for both enzymatic and non-enzymatic reactions. Non-enzymatic reaction rates serve as backgrounds and were subtracted in all cases. For analogs whose enzymatic reaction was detectable, their k_{cat} and $K_{m(apparent)}$ values were measured. For this purpose, *N*-haloacetyltryptamine substrate concentrations ranging from 0.5 to 8.0 mM (but 0.5–4.0 mM for **5**, and 0.05–1.0 mM for **6** due to low solubility) were employed in the presence of fixed and near-saturating CoASH (2 mM). 0.5–1.0 µM of AANAT were employed, and the assay reactions were run for 2 min at 30°C. Rate measurements were made under initial conditions, i.e. limiting substrate turnover was maintained at $\leq 10\%$. All measurements were made in duplicate and data agreed within 20% in each duplicate run. Enzyme activity was linear with AANAT concentration. Kinetic parameters (k_{cat} and $K_{m(apparent)}$) were calculated by fitting the data into the Michaelis–Menten equation using a non-linear least squares approach with the computer program Kaleidagraph™ (Reading, PA, USA), and the values are recorded as mean ± S.E.M. in Table 1.

4.7. [Y168F]-AANAT mutant studies

The [Y168F]-AANAT DNA (independently prepared by Hickman et al. [38]) was obtained using the QuikChange Kit (Stratagene™) and the mutation confirmed by DNA sequencing of the entire open reading frame. The protein was expressed and purified as the GST fusion construct as described previously [18]. Kinetic assays were carried out as described above for the wild-type AANAT. The apparent k_{cat} values were determined at saturating concentrations (2 mM, $> 3K_m$) of each substrate (demonstrated for reaction with **2** and CoASH) and are shown in the text. Precise K_m values were difficult to measure because of signal-to-noise limitations but were < 0.7 mM for **2** and CoASH.

4.8. Two-substrate kinetic studies

CoASH and *N*-chloroacetyltryptamine (**4**) were employed in the two-substrate kinetic analysis. The k_{cat} and K_m measurements were made for CoASH (concentration range of 0.1–2.0 mM) at three different fixed concentrations (0.5, 1.0, and 2.0 mM) of substrate **4**. Alkyltransferase assays were performed as described above and in [24]. A concentration of 1.0 µM of AANAT was employed. Data were fitted into the sequential (ternary complex) mechanism equation (Eq. 1) using a non-linear least squares approach with the computer program KinetAsyst II™ (IntelliKinetics, State College, PA, USA) based on the Cleland algorithms [44]. Kinetic parameters are recorded as mean ± S.E.M. in Fig. 4. $K_a = K_m$ of CoASH, K_{ia} = dissociation constant for CoASH to

free enzyme, $K_b = K_m$ of *N*-chloroacetyltryptamine (**4**). Fitting to a ping-pong mechanism gave a larger sum of squares of the residuals and larger S.E.M. values:

$$V = V_m AB/(K_{ia}K_b + K_a B + K_b A + AB) \quad (1)$$

4.9. Product inhibition studies

Bisubstrate analog **7** was employed as a product inhibitor in the product inhibition analyses which were performed with CoASH and analog **4** as the enzyme substrates. On the HPLC chromatograms, analog **7** was well separated from analog **1** which is the direct product for the reaction between CoASH and substrate **4**. The k_{cat} and K_m measurements were made for CoASH (concentration range of 0.05–2.0 mM) at a fixed substrate **4** concentration (4.0 mM) and three different fixed concentrations (0, 12, and 25 μM) of the bisubstrate analog **7**, as well as for substrate **4** (concentration range of 0.5–8.0 mM) at a fixed CoASH concentration (2.0 mM) and three different fixed concentrations (0, 12, and 24 μM) of the bisubstrate analog **7**. Alkyltransferase assays were performed as described above and in [24]. A concentration range of 0.5–1.0 μM of AANAT was employed. All the data points for an individual experiment were first fitted to the equations for all three inhibition patterns, i.e. linear competitive (Eq. 2), linear non-competitive (Eq. 3), and linear uncompetitive inhibition (Eq. 4) using a non-linear least squares approach with the computer program KinetAsyst II™ (IntelliKinetics, State College, PA, USA) based on the Cleland algorithms [44]. The $K_{ii} = K_i$ intercept and $K_{is} = K_i$ slope. The best fit for a single data set was one having the smallest S.E.M. values and the sum of the squares of the residuals:

$$V = V_m S/[K_m(1 + I/K_{is}) + S] \quad (2)$$

$$V = V_m S/[K_m(1 + I/K_{is}) + S(1 + I/K_{ii})] \quad (3)$$

$$V = V_m S/[K_m + S(1 + I/K_{ii})] \quad (4)$$

4.10. Rate versus pH profile studies

CoASH and *N*-chloroacetyltryptamine (**4**) were employed in the rate versus pH profile analysis. The k_{cat} and K_m measurements were made for CoASH (concentration range of 0.1–2.0 mM) at fixed substrate **4** concentration (8.0 mM), as well as for substrate **4** (concentration range of 0.5–8.0 mM) at fixed CoASH concentration (2.0 mM) in the pH range 6.0–8.2. Alkyltransferase assays were performed as described above and in [24]. At each pH investigated, enzyme activities were shown to be linear for at least 4 min and standard Michaelis–Menten kinetic behavior was observed. All assay reactions were initiated with the addition of substrate **4**. A concentration range of 0.1–3.0 μM of AANAT was employed. The following buffers were used to obtain the desired pH values: MES for pH 6.0 and 6.4; sodium phosphate for pH 6.8; MOPS for pH 7.4; EPPS for pH 8.2. The k_{cat} and k_{cat}/K_m data were fitted into Eqs. 5 and 6, respectively, where H is the proton concentration, and K_1 is the dissociation constant for an ionizable group from enzyme or substrate that facilitates the reaction in its deprotonated form [41]:

$$\log(k_{cat})_{app} = \log(k_{cat}/(1 + H/K_1)) \quad (5)$$

$$\log(k_{cat}/K_m)_{app} = \log(k_{cat}/K_m/(1 + H/K_1)) \quad (6)$$

4.11. AANAT acetyltransferase inhibition studies of *N*-haloacetyltryptamines

Acetyltransferase activity was measured as described previously using a spectrophotometric assay in which CoASH levels were determined indirectly by monitoring its reaction product with DTNB at 412 nm [18]. Assay reactions (pH 6.8) containing acetyl-CoASH (1.0 mM), tryptamine (1.0 mM), and *N*-haloacetyltryptamines (varied around IC_{50}) were initiated with AANAT and the reactions were allowed to proceed for 2 or 4 min at 30°C before quenching with a 3.2 M aqueous guanidinium hydrochloride solution (pH 6.8). Rate measurements were made under initial conditions, i.e. limiting substrate turnover ≤ 10%. All measurements were made in duplicate and data agreed within 20% in each duplicate run. A background (quenched before adding AANAT) was run for each inhibitor concentration. From non-linear plots of rate versus inhibitor concentration, an IC_{50} was obtained for each inhibitor as an indicator of the potency (Table 2).

4.12. Pineal cell culture AANAT inhibition studies

N-Chloroacetyltryptamine (**4**) was studied for its in vivo inhibitory effects on AANAT acetyltransferase activity and melatonin levels. Assays were conducted essentially as described previously [24]. Data are shown in Table 3.

Acknowledgements

This work was supported in part by the Ellison Medical Foundation and the NIH. We thank Dr. Paul Thompson and Dr. Ehab Khalil for helpful discussions. The NMR studies were performed in the Biochemistry NMR Facility at Johns Hopkins University, which was established by a grant from the National Institutes of Health (GM 27512) and a Biomedical Shared Instrumentation Grant (1S10-RR06262-0).

References

[1] D.C. Klein, J.L. Weller, Indole metabolism in the pineal gland: a circadian rhythm in *N*-acetyltransferase, Science 169 (1970) 1093–1095.

[2] S.L. Coon, P.H. Roseboom, R. Baler, J.L. Weller, M.A.A. Namboodiri, E.V. Koonin, D.C. Klein, Pineal serotonin *N*-acetyltransferase: expression cloning and molecular analysis, Science 270 (1995) 1681–1683.

[3] J. Borjigin, M.M. Wang, S.H. Snyder, Diurnal variation in mRNA encoding serotonin *N*-acetyltransferase in pineal gland, Nature 378 (1995) 783–785.

[4] D.C. Klein, P.H. Roseboom, S.L. Coon, New light is shining on the melatonin rhythm enzyme, Trends Endocrinol. Metab. 7 (1996) 106–112.
[5] D.C. Klein, S.L. Coon, P.H. Roseboom, J.L. Weller, M. Bernard, J.A. Gastel, M. Zatz, P.M. Iuvone, I.R. Rodriquez, V. Begay, J. Falcon, G.M. Cahill, V.M. Cassone, R. Baler, The melatonin rhythm-generating enzyme: molecular regulation of serotonin *N*-acetyltransferase in the pineal gland, Recent Prog. Horm. Res. 52 (1997) 307–357.
[6] J. Arendt, Melatonin and the Mammalian Pineal Gland, Chapman and Hall, New York, 1995.
[7] W. Pierpaoli, W. Regelson, C. Colman, The Melatonin Miracle. Nature's Age-reversing, Disease-fighting, Sex-enhancing Hormone, Pocket Books, New York, 1995.
[8] S.M. Reppert, D.R. Weaver, Melatonin madness, Cell 83 (1995) 1059–1062.
[9] H. Iguchi, K. Kato, H. Ibayashi, Age-dependent reduction in serum melatonin concentrations in healthy human subjects, J. Clin. Endocrinol. Metab. 55 (1982) 27–29.
[10] T. Akerstedt, J.E. Froberg, W. Friberg, L. Wetterberg, Melatonin excretion, body temperature and subjective arousal during 64 hours of sleep deprivation, Psychoneuroendocrinology 4 (1979) 219–225.
[11] A.J. Lewy, R.L. Sack, L.S. Miller, T.M. Hoban, Antidepressant and circadian phase-shifting effects of light, Science 235 (1987) 352–354.
[12] G.J. Maestroni, A. Conti, W. Pierpaoli, Role of the pineal gland in immunity. III. Melatonin antagonizes the immunosuppressive effect of acute stress via an opiatergic mechanism, Immunology 63 (1988) 465–469.
[13] H.J. Harlow, Influence of the pineal gland and melatonin on blood flow and evaporative water loss during heat stress in rats, J. Pineal Res. 4 (1987) 147–159.
[14] M. Cohen, M. Lippman, B. Chabner, Role of pineal gland in aetiology and treatment of breast cancer, Lancet ii (1978) 814–816.
[15] A.F. Neuwald, D. Landsman, GCN5-related histone *N*-acetyltransferases belong to a diverse superfamily that includes the yeast SPT10 protein, Trends Biochem. Sci. 22 (1997) 154–155.
[16] F. Javier Teran, M. Alvarez, J.E. Suarez, M.C. Mendoza, Characterization of two aminoglycoside-(3)-*N*-acetyltransferase genes and assay as epidemiological probes, J. Antimicrob. Chemother. 28 (1991) 333–346.
[17] D.E. Sterner, S.L. Berger, Acetylation of histones and transcription-related factors, Microbiol. Mol. Biol. Rev. 64 (2000) 435–459.
[18] J. De Angelis, J. Gastel, D.C. Klein, P.A. Cole, Kinetic analysis of the catalytic mechanism of serotonin *N*-acetyltransferase (EC 2.3.1.87), J. Biol. Chem. 273 (1998) 3045–3050.
[19] K.G. Tanner, R.C. Trievel, M.-H. Kuo, R.M. Howard, S.L. Berger, C.D. Allis, R. Marmorstein, J.M. Denu, Catalytic mechanism and function of invariant glutamic acid 173 from the histone acetyltransferase GCN5 transcriptional coactivator, J. Biol. Chem. 274 (1999) 18157–18160.
[20] O.D. Lau, A.D. Courtney, A. Vassilev, L.A. Marzilli, R.J. Cotter, Y. Nakatani, P.A. Cole, p300/CBP-associated factor histone acetyltransferase processing of a peptide substrate. Kinetic analysis of the catalytic mechanism, J. Biol. Chem. 275 (2000) 21953–21959.
[21] K.G. Tanner, M.R. Langer, Y. Kim, J.M. Denu, Kinetic mechanism of the histone acetyltransferase GCN5 from yeast, J. Biol. Chem. 275 (2000) 22048–22055.
[22] K.G. Tanner, M.R. Langer, J.M. Denu, Kinetic mechanism of human histone acetyltransferase P/CAF, Biochemistry 39 (2000) 11961–11969.
[23] E.M. Khalil, P.A. Cole, A potent inhibitor of the melatonin rhythm enzyme, J. Am. Chem. Soc. 120 (1998) 6195–6196.
[24] E.M. Khalil, J. De Angelis, M. Ishii, P.A. Cole, Mechanism-based inhibition of the melatonin rhythm enzyme: pharmacologic exploitation of active site functional plasticity, Proc. Natl. Acad. Sci. USA 96 (1999) 12418–12423.
[25] J.D. Robishaw, J.R. Neely, Coenzyme A metabolism, Am. J. Physiol. 248 (1985) E1–E9.
[26] J.F.A. Chase, P.K. Tubbs, Conditions for the self-catalyzed inactivation of carnitine acetyltransferase, Biochem. J. 111 (1969) 225–235.
[27] J.F.A. Chase, P.K. Tubbs, Specific inhibitors of carnitine acetyltransferase and other acyltransferases, Biochem. J. 100 (1966) 47P–48P.
[28] J.W. Williams, D.B. Northrop, Synthesis of a tight-binding, multisubstrate analog inhibitor of gentamicin acetyltransferase I, J. Antibiot. 32 (1979) 1147–1154.
[29] T.H. Lowry, K.S. Richardson, Mechanism and Theory in Organic Chemistry, Harper and Row, New York, 1981.
[30] D.S. Noyce, J.A. Virgilio, The synthesis and solvolysis of 1-phenylethyl disubstituted phosphinates, J. Org. Chem. 37 (1972) 2643–2647.
[31] S.D. Ross, M. Finkelstein, R. Petersen, Rates and salt effects in the reactions of phenacyl bromide with *N*-ethylaniline and triethylamine in chloroform, J. Am. Chem. Soc. 90 (1968) 6411–6415.
[32] A. Halvorsen, J. Songstad, The reactivity of 2-bromo-1-phenylethanone (phenacyl bromide) toward nucleophilic species, J. Chem. Soc. Chem. Commun. (1978) 327–328.
[33] R.N. Armstrong, Glutathione *S*-transferases: structure and mechanism of an archetypical detoxication enzyme, Adv. Enzymol. Relat. Areas Mol. Biol. 69 (1994) 1–44.
[34] I. Ahmad, D.N. Rao, Chemistry and biology of DNA methyltransferases, Crit. Rev. Biochem. Mol. Biol. 31 (1996) 361–380.
[35] F.L. Zhang, P.J. Casey, Protein prenylation: molecular mechanisms and functional consequences, Annu. Rev. Biochem. 65 (1996) 241–269.
[36] A.C. Brouwer, J.F. Kirsch, Investigation of diffusion-limited rates of chymotrypsin reactions by viscosity variation, Biochemistry 21 (1982) 1302–1307.
[37] J. Kyte, Mechanism in Protein Chemistry, Garland, New York, 1995.
[38] A.B. Hickman, M.A. Namboodiri, D.C. Klein, F. Dyda, The structural basis of ordered substrate binding by serotonin *N*-acetyltransferase: enzyme complex at 1.8 Å resolution with a bisubstrate analog, Cell 97 (1999) 361–369.
[39] I. Segel, Enzyme Kinetics, Wiley, New York, 1975.
[40] Merck and Co., The Merck Index, 12th edn., 1996, p. 2531.
[41] M. Dixon, E.C. Webb, Enzymes, Academic Press, New York, 1964.
[42] E.M. Khalil, J. De Angelis, P.A. Cole, Indoleamine analogs as probes of the substrate selectivity and catalytic mechanism of serotonin *N*-acetyltransferase, J. Biol. Chem. 273 (1998) 30321–30327.
[43] R.B. Silverman, The Organic Chemistry of Drug Design and Drug Action, Academic Press, San Diego, CA, 1992.
[44] W.W. Cleland, Statistical analysis of enzyme kinetic data, Methods Enzymol. 63 (1979) 103–138.